Jurnal Polimesin
Department of Mechanical Engineering
State Polytechnic of Lhokseumawe
http://e-jurnal.pnl.ac.id/polimesin
e-ISSN : 2549-1199 No. : 3 Month : June
p-ISSN : 1693-5462 Volume : 23 Year : 2025

Processing dates: received on 2025-03-31, reviewed on 2025-05-07, accepted on 2025-05-23 and online availability on 2025-06-30

Experimental investigation of the impact of non-uniform pipe diameters on natural circulation and dimensionless flow in in a rectangular loop

Iwan Roswandi[1,2], Agus Sunjarianto Pamitran[1,*], Mulya Juarsa[2], Arif Adtyas Budiman[2]

[1]Department of Mechanical Engineering, University of Indonesia, Depok 16424, Indonesia

[2]Nuclear Reactor Therma-Fluids System Research Group, Research Center of Nuclear Reactor Technology, National Research and Innovation Agency, Serpong 15310, Indonesia

*Corresponding author: pamitran@eng.ui.ac.id

Abstract

This experimental study investigates the effect of non-uniform pipe diameters on natural circulation flow within a rectangular loop related to non-dimensional numbers, such as the Reynolds number and the Grashof modified number. The study aims to understand how variations in pipe diameters influence natural circulation, which is critical for thermal engineering applications, including passive cooling systems for nuclear reactors and thermal management in electronic devices. In this study, a loop system with varying pipe diameters operates without a pump at atmospheric pressure. Data on fluid flow and temperature distribution were recorded at different temperature settings. The results show that fluid flow increases with temperature, decreasing fluid density and enhancing buoyancy forces. This increases the Reynolds number, reaching turbulent flow at 70°C throughout the loop. However, the 2-inch diameter hot leg remains in the transition region up to 90°C. The experimental correlation shows higher Grashof modified numbers than previous models, highlighting the significant impact of pipe diameter variations on buoyancy forces and flow transitions. These findings emphasize the importance of non-uniform pipe geometries in influencing natural circulation flow and its transition from laminar to turbulent flow, providing valuable insights for designing systems with non-uniform pipe configurations.

Keywords:
Natural circulation, non-uniform diameter, Reynolds number, rectangular loop, buoyancy force.

1 Introduction

Natural circulation in rectangular loops has become the focus of numerous studies due to its crucial role in engineering applications, such as heat exchangers, passive cooling systems for nuclear reactors, and thermal management in electronic devices. Unlike forced circulation, which relies on mechanical pumps, natural circulation utilizes buoyancy forces generated by temperature differences within the loop. This phenomenon is of particular interest because it enables fluid movement without external energy input, making it an efficient solution for systems that require passive heating or cooling.

A rectangular loop is one of the experimental facility models designed to simulate a passive cooling system based on natural circulation. In this system, the temperature difference between the heating section (hot leg) and the cooling section (cold leg) creates a density gradient that triggers the natural movement of the fluid. This mechanism enables continuous heat transfer within the loop, allowing the system to maintain thermal stability without the need for additional energy. Therefore, a comprehensive understanding of the thermohydraulic characteristics of this loop configuration—particularly the influence of geometric variations such as pipe diameter—is essential for enhancing the efficiency and effectiveness of passive cooling system designs across various engineering applications.

Prior research has established a robust foundation for understanding natural circulation dynamics. Regarding loop geometry and component orientation, Vijayan et al. [1] demonstrated that vertical heater–vertical cooler (VHVC) configurations yield the most stable flow. Their work further revealed that smaller-diameter loops tend to exhibit better stability [2]. Garibaldi et al. [3] investigated the influence of loop geometry and fluid properties on thermal performance, showing that FC-43 fluid transfers heat less efficiently than water. Misale et al. [4] emphasized that a 75° inclination angle in rectangular loops enhances flow stability. Hariyanto et al. [5] observed temperature variations between loops even in identically designed VHVC systems, a finding corroborated by Misale et al. [6], who confirmed the continued validity of Vijayan's stability correlations for interconnected small-scale loops. Vijayan et al. [1] established the relationship between Reynolds number and Grashof modified number per geometry ratio (Gr_m/N_G) as key stability prediction parameters. Swapnalee et al. [7] expanded this work by developing stability maps for laminar, transitional, and turbulent flow regimes, consistent with Vijayan's findings. Kumar et al. [8] refined the approach through improved correlations based on higher-precision experimental data.

Several studies have highlighted flow instability and oscillation characteristics. Saha et al. [9] documented periodic flow oscillations at moderate power levels, while Misale et al. [10] reported increasing oscillation frequency and amplitude with rising power input. Seyyedi et al. [11] demonstrated that asymmetric heater positioning and reduced inclination angles enhance flow stability. For systems featuring auxiliary components or interconnected loops, thermal performance and flow stability remain critical research foci. Misale et al. [12] revealed that thermal feedback in coupled loops improves thermal performance, particularly at elevated coolant temperatures. Elton et al. [13] observed stable single-phase flow at power levels up to 100 kW, whereas Bello et al. [14] recorded increased flow rates with temperature in VHHC configurations. Elton et al. [15,16] additionally investigated orifice plates, determining that minimal diameters optimize flow stability.

These studies have provided insights into natural circulation in loops with uniform diameters. However, there is still a gap in understanding the impact of non-uniform diameters. Non-dimensional numbers such as Reynolds number, Grashof modified number, and geometric ratio (N_G) have proven effective in predicting flow regimes and circulation stability. In real-world applications, such as the passive core cooling system of the AP1000 nuclear reactor, variations in pipe diameters are implemented to optimize fluid transport and thermal response under natural circulation conditions [17]. Based on experimental results, this study aims to investigate the influence of non-uniform diameter on non-dimensional numbers in natural circulation within rectangular loops, providing new insights for practical applications in thermal engineering.

2 Methodology

2.1 Experimental procedure

The experimental system designed to study the non-dimensional numbers in natural circulation fluid utilizes a non-uniform diameter rectangular loop that does not require a pump for circulation, operating under atmospheric pressure conditions. This design mimics practical implementations such as the AP1000 nuclear reactor, which employs a larger diameter in the hot leg compared to the cold leg to enhance buoyancy-driven flow and improve thermal performance under passive cooling conditions. In this study, several experimental parameters were defined to investigate the effect of temperature on natural circulation in a rectangular loop, as presented in Table 1. Each experiment was conducted with different

temperature variations, ranging from 50°C to 90°C. One of the main considerations in selecting this temperature range was to ensure that the system remained above room temperature while maintaining a single-phase (liquid) condition at atmospheric pressure (1 atm). The choice of this temperature range aims to avoid reaching the saturation temperature of water, which could lead to a phase transition from liquid to vapor. Such a phase change could affect the natural circulation mechanism as well as the observed parameters. By limiting the temperature to a maximum of 90°C, the experiments can be consistently conducted in a pure liquid state, ensuring the validity of the data and making the results more relevant for applications in single-phase natural circulation systems.

Table 1. Experimental parameters

Temp. Setting (°C)	Dia. Cold leg (inch)	Dia. Hot leg (inch)	Temp. WCT (°C)	Flowrate WCT (LPM)	Steady State Time (s)	Repetition (time)
50	1	2	10	10	3600	3
60	1	2	10	10	3600	3
70	1	2	10	10	3600	3
80	1	2	10	10	3600	3
90	1	2	10	10	3600	3

The experimental setup uses corrosion-resistant materials capable of handling fluids above 100°C. The system has a data acquisition system that monitors fluid temperature and flow in real time. The loop is constructed from 304 stainless steel pipes with an outer diameter of 1 inch and a thickness of 2.77 mm, except for the hot-leg pipe, which has a 2-inch diameter and a thickness of 2.77 mm. Temperature distribution in the loop is monitored using K-type thermocouples (accuracy ±0.5%) installed at various points along the system to measure temperature variations comprehensively

The experiment uses the Water Heating Tank (WHT) and the Water-Cooling Tank (WCT). The WHT is positioned at the bottom of the loop and is equipped with eight immersion heaters, each with a power of 700 W, which directly heat the fluid. The WCT employs a shell and tube system assisted by a Control Thermostatic Bath (CTB) to maintain the coolant temperature at 10°C, with a coolant circulation rate of 10 LPM. The fluid used is tap water, which is heated in the WHT and cooled in the WCT, creating natural circulation in the loop. The fluid flow rate is measured using a magnetic flowmeter with an accuracy of ±0.5%, enabling precise flow measurements without needing a recirculation pump, as shown in Fig. 1.

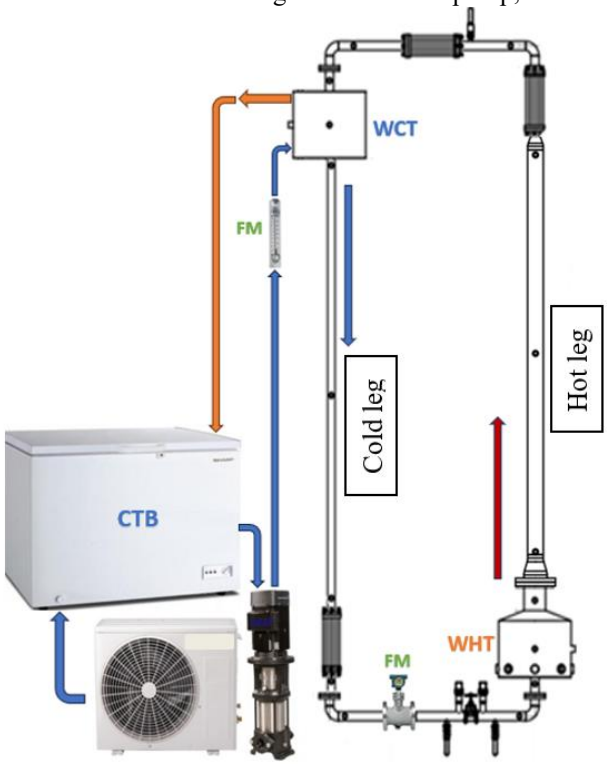

Fig. 1. Experimental setup

The experimental procedure begins by cooling the fluid in the WCT to 10°C, then heating it in the WHT until the target temperature, ranging from 50°C to 90°C, is reached. Once the temperature in the WHT reaches the target, the Solid-State Relay (SSR) control system automatically regulates the heater's on/off status to maintain a constant temperature. This process is sustained for one hour to ensure steady-state conditions. Temperature distribution measurements and fluid flow are taken over three trials to ensure stable and accurate data under natural circulation conditions. All operations using instrumentation and control during the experiment are shown in Fig. 2, and the experimental parameters are shown in Table 1.

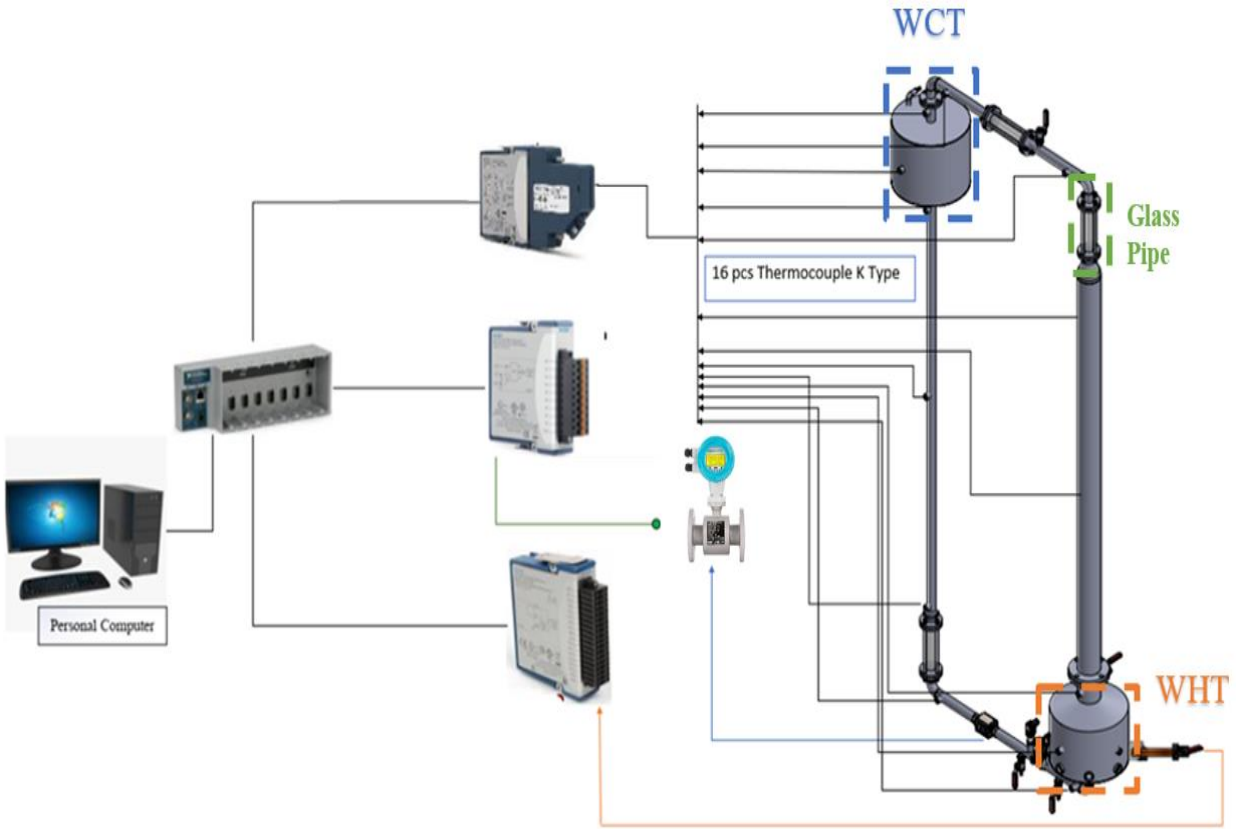

Fig. 2. Instrumentation diagram

2.2 Analysis

After the experiment, the next step was to analyse the obtained data. The first phase of this analysis involves examining the changes in fluid properties due to the increase in temperature during the experiment. Fluid properties play a crucial role in determining the behaviour of natural circulation, as they influence buoyancy forces, viscosity, and the fluid's ability to transfer heat. A correlation developed by Crabtree and Siman-Tov [18], with an accuracy of 0.3%, was used to analyse these fluid properties. Several fluid properties relevant to the study of natural circulation include *The specific heat capacity (c_p) is calculated using following Eq. (1).*

$$c_p = 1000 \times \left[\frac{A+CT}{1+BT+DT^2}\right]^{1/2} \quad (1)$$

where, c_p = specific heat capacity (J/kg°C), T = Temperature (ºC), A = 17.48908904, B = -1.67507x10^{-3}, C = -0.03189591, D = -2.8748x10^{-6}. The dynamic viscosity (μ) is calculated using the following Eq. (2).

$$\mu = exp\left[\frac{A+CT}{1+BT+DT^2}\right] \quad (2)$$

where, μ = dynamic-viscosity (Pa.s), A= -6.325203964, B=8.705317x10^{-3}, C= -0.088832314, D= -9.657x10^{-7}. The density of water is ρ (kg/m³) is calculated using Eq. (3).where, A= 1004.789042, B= -0.046283, C = -7.9739, T_F = 1,8T+32. The next step is to determine the non-dimensional numbers using the following correlations.

$$\rho = A + BT_F + CT_F^2 \quad (3)$$

The Grashof number represents the ratio of buoyant force to viscous force in natural convection fluid flow. In studies of natural circulation, Vijayan et al. developed the Grashof modified number as fig (4). where, D = loop diameter (m), Q_h = total heater heat input (W), Δz = distance between heater and cooler (m), β = thermal expansion coefficient (1/°C), and A = cross-sectional area through which the fluid flows (m²)

$$Gr_m = \frac{D^3\rho^2 g\beta Q_h \Delta z}{ACp\mu^3} \quad (4)$$

The Reynolds number is dimensionless, indicating the flow regime based on the ratio of inertial force to viscous force in the fluid. Flow regimes are classified as laminar (Re < 2100), transition (2100 < Re < 4000), and turbulent (Re > 4000). The Reynolds number can be calculated using Eq. (5), Munson et al. [18].

$$R_e = \frac{Inertia\ force}{Viscosity\ force} = \frac{v_s D}{v} = \frac{\rho v_s D}{\mu} = \frac{\rho QD}{\mu A} \quad (5)$$

where Q = flow rate (m^3/s) and the Geometric Ratio (N_G) is the ratio of the total loop length to the average hydraulic diameter of the pipe (L/D), influenced by head loss due to friction factors. Regarding non-uniform diameter loops, Vijayan et al. [20] provided the following Eq. (6).where L_t is the total length of the circulation loop (m), D (m) is the average hydraulic diameter, K is the pressure loss coefficient for minor losses at elbows (-), and f is the friction factor (-).

$$N_G = \sum \frac{L}{D} + \frac{\sum k}{f} \quad (6)$$

This method allows for the accurate calculation of non-dimensional numbers crucial in characterizing and understanding the flow behaviour and heat transfer in natural circulation systems with non-uniform diameters.

3 Results and Discussion

The steady-state experiment was conducted for 3600 seconds and repeated three times for each loop configuration to ensure the accuracy and consistency of the obtained data. The fluid flow pattern and temperature distribution at steady-state conditions were also systematically recorded, allowing the data to be processed and presented in tables and graphs to support a comprehensive thermohydraulic analysis.

The experimental results in Table 2 and Fig. 3 demonstrate that the immersion heater successfully maintains the temperature set in the WHT and at other points within the system. The average temperature at the WHT increases linearly with the temperature setting, confirming the heater's effectiveness in maintaining the desired temperature. At the 50°C setting, the WHT temperature was recorded at 50.71°C, rising to 90.53°C at the 90°C setting. This increase in temperature at the WHT reflects the immersion heater's ability to maintain the target temperature.

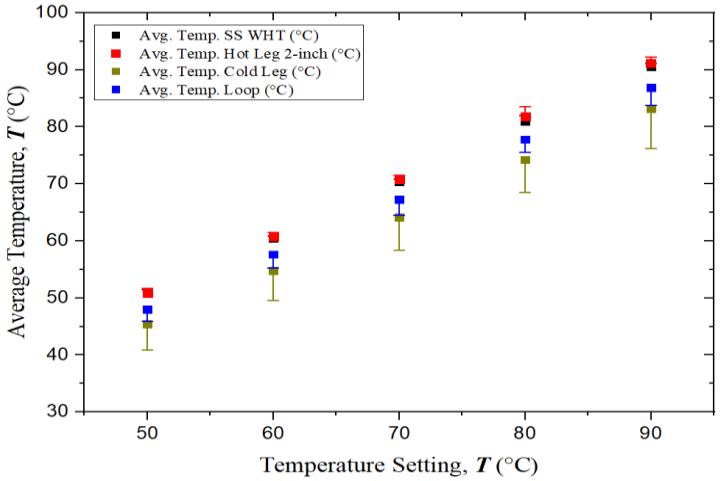

Fig. 3. Deviation to temperature setting

Table 2. Steady-state experiment results for 3600 seconds

Temp. Setting (°C)	Avg. Temp. SS WHT (°C)	Avg. Temp. Hot leg 2-inch (°C)	Avg. Temp. Cold leg (°C)	Avg. Temp. Loop (°C)	Avg. Flowrate, Q (lpm)
50	50.71	50.86	45.41	47.97	1.75
60	60.43	60.72	54.77	57.61	2.05
70	70.40	70.74	64.16	67.26	2.29
80	80.98	81.74	74.23	77.77	2.57
90	90.53	91.12	83.11	86.89	2.78

Similarly, the hot leg 2-inch temperature follows a similar upward trend. The temperature at the Hot Leg is consistently slightly higher than the WHT, with an average difference of approximately 0.15°C at each temperature setting. This phenomenon can be explained by the heat transfer process, where the fluid heated in the WHT flows towards the hot leg, transferring most of its heat to the fluid passing through that section. At the 50°C setting, the average temperature of the hot leg was 50.86°C, and at the 90°C setting, the temperature reached 91.12°C.

Meanwhile, the temperature at the cold leg emphasizes the role of the WCT in absorbing heat from the loop. The temperature difference between the cold and hot legs indicates how effectively the WCT cools the fluid. At the 50°C setting, the average temperature at the cold leg was 45.41°C, with a 6.4°C difference from the Hot Leg temperature. This difference also grows as the WHT temperature increases, with the cold leg temperature reaching 83.11°C at the 90°C setting. This shows that as the WHT temperature increases, the WCT absorbs heat from the circulating fluid more efficiently.

Additionally, the fluid flow rate increases as the temperature setting rises. At the 50°C setting, the flow rate was measured at 1.75 LPM, which increased to 2.77 LPM at the 90°C setting. This increase in flow rate can be attributed to the buoyancy forces in the natural circulation system. As the fluid temperature increases, its density decreases, leading to a larger temperature difference between the hot and cold legs. This difference induces buoyancy forces that push the fluid upward, thus increasing the flow rate in the system. This demonstrates the direct relationship between temperature and flow rate, where higher temperatures generate stronger buoyancy forces, resulting in a higher fluid flow rate. Fluid properties steady-state experiment results in Table 3.

Table 3. Fluid properties steady-state experiment results

Temp. Setting (°C)	ρ Loop (kg/m³)	ρ Hot Leg 2-inch (kg/m³)	μ Loop x 10^{-4} (Pa.s)	μ Hot leg 2-inch x 10^{-4} (Pa.s)	c_P Loop (J/kg°C)	c_P Hot leg (J/kg.°C)
50	988.14	986.9	5.6	5.3	4180.82	4181.71
60	983.83	982.33	4.8	4.5	4184.27	4185.69
70	979.02	977.17	4.1	3.9	4189.18	4191.31
80	973.24	970.92	3.6	3.4	4196.27	4199.44
90	967.77	965.08	3.2	3.1	4204	4208.12

Table 3 shows the variation in fluid properties—density (ρ), dynamic viscosity (μ), and specific heat capacity (c_P)—for the loop and the 2-inch hot leg sections at different temperature settings. As the temperature increases from 50°C to 90°C, the water density inside both the loop and the hot leg decreases as expected due to the thermal expansion of the fluid. The water density inside the loop decreases from 988.14 kg/m³ at 50°C to 967.77 kg/m³ at 90°C, and similarly, the hot leg density decreases from 986.9 kg/m³ at 50°C to 965.08 kg/m³ at 90°C. However, the water density inside the hot leg is consistently slightly lower than in the loop, which can be attributed to the larger diameter of the hot leg (2 inches), causing it to experience slightly different thermal conditions and density changes compared to the rest of the loop.

Regarding dynamic viscosity (μ), both the loop and the 2-inch hot leg exhibit a similar decreasing trend with rising temperature. The viscosity in the loop decreases from 5.6×10^{-4} Pa·s at 50°C to 3.2×10^{-4} Pa·s at 90°C, while in the 2-inch hot leg, it declines from 5.3×10^{-4} Pa·s to 3.1×10^{-4} Pa·s over the same temperature range. The slightly lower viscosity observed in the larger-diameter hot leg—approximately 0.1 to 0.3×10^{-4} Pa·s lower than in the loop—can be interpreted using the dynamic viscosity Eq. (2). This formulation highlights the strong dependence of viscosity on temperature, where increasing temperature reduces molecular cohesion, thereby lowering viscosity. Nevertheless, the consistent difference between the two sections suggests that geometric factors also play a significant role. The larger pipe diameter tends to support more stable flow, reduce wall shear stress, and minimize localized turbulence, thus promoting more laminar-like behavior. These flow characteristics may contribute to the slightly lower effective viscosity recorded in the hot leg. Overall, both temperature and geometry jointly influence the fluid's viscous behavior, which in turn affects the efficiency of flow and heat transfer within the system.

In terms of specific heat capacity (Cp), both the loop and the hot leg show similar increases with temperature, from 4180.82 J/kg°C at 50°C to 4204 J/kg°C at 90°C in the loop and from 4181.71 J/kg°C at 50°C to 4208.12 J/kg°C at 90°C in the hot leg. The hot leg's Cp values are slightly higher than all temperatures along the loop, suggesting that the hot leg may have a slightly higher capacity for storing heat, which could contribute to more efficient thermal management in that section.

These changes in fluid properties—reduced viscosity, decreased density, and slightly increased specific heat—align with basic principles of thermal dynamics. The lower viscosity, density, and increased buoyancy forces lead to faster fluid flow, as observed in the increased mass flow rate at higher temperatures. Moreover, the differences in properties between the loop and the hot leg suggest that the hot leg, with its larger diameter, might experience slightly better flow characteristics, enhancing its efficiency in both fluid movement and heat transfer. The role of dynamic viscosity, Reynolds number, and modified Grashof number in the mechanism of natural circulation system is shown in Fig. 4.

Fig. 4 illustrates that dynamic viscosity Reynolds number and Grashof modified number in a natural circulation system. The available data shows that a decrease in dynamic viscosity leads to an increase in both Reynolds number and Grashof modified number, both in the loop and the 2-inch hot leg. However, the difference in diameter between the loop and the 2-inch hot leg affects the tendency of the Reynolds number and the Grashof modified number to change. The fluid velocity is higher in the loop, with a smaller diameter, resulting in a greater Re than the 2-inch hot leg.

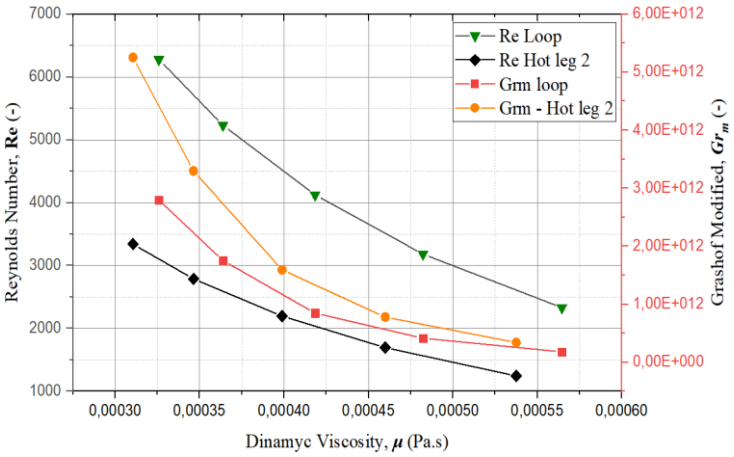

Fig. 4. Effect of dynamics viscosity to Re and Gr_m

In contrast, although viscosity decreases in the 2-inch hot leg, the Reynolds number remains smaller because the larger cross-sectional area reduces the fluid velocity. From the available data, when the viscosity decreases from $5.65\text{x}10^{-4}$ Pa.s to $3.26\text{x}10^{-4}$ Pa.s, the Reynolds number in the loop increases from 2330.16 to 6279.25. In contrast, in the 2-inch hot leg, when the viscosity decreases from $5.37\text{x}10^{-4}$ Pa.s to $3.11\text{x}10^{-4}$ Pa.s, the Reynolds number only increases from 1243.43 to 3341.35.

On the other hand, the Grashof modified number value in the 2-inch hot leg is higher than in the loop, indicating that buoyancy forces are more dominant in the hot leg. The 2-inch diameter allows for a more significant temperature gradient within the fluid, enhancing the density difference and leading to stronger buoyancy forces than the loop. In the loop, Grashof modified number increases from 1.80E+11 to 2.79E+12, while in the 2-inch hot leg, Grashof modified number increases even more, from 3.39E+11 to 5.25E+12. This shows that the 2-inch hot leg relies more on buoyancy forces than fluid inertia to maintain flow in a natural circulation system. At the same time, the loop tends to be more influenced by fluid momentum.

The increase in Reynolds and Grashof modified numbers directly affects heat transfer within the system. As the Reynolds number increases, the fluid flow becomes more developed, which leads to more effective heat transfer due to improved fluid mixing. Meanwhile, the increase in Grashof modified number indicates that the density difference due to the temperature gradient becomes larger, making the buoyancy forces more effective in driving heat transfer. Heat transfer tends to be influenced in the loop by a combination of momentum and buoyancy effects. In contrast, in the 2-inch hot leg, buoyancy becomes the dominant factor in the heat transfer process. The increase in Reynolds number in the flow series is shown in Fig. 5.

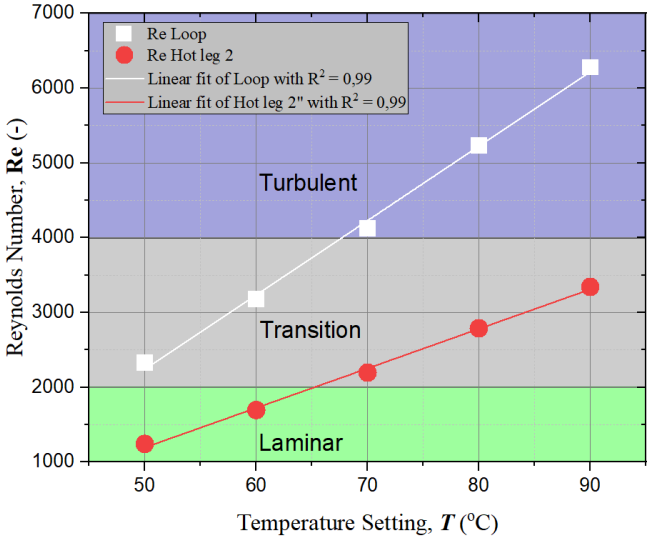

Fig. 5. Reynolds Number Experiment

Fig. 5 shows regarding pressure drop, the increase in Reynolds number in the loop indicates that fluid friction against the pipe walls decreases relative to fluid momentum, leading to a smaller pressure loss due to friction. Although pressure was not measured directly in the experimental setup—since no pressure transducer was installed—this interpretation is supported by fluid dynamics theory. As the Reynolds number increases, the flow transitions from laminar to turbulent, and the relative contribution of viscous forces to flow resistance diminishes. According to the Darcy–Weisbach equation and the Moody diagram, the friction factor decreases with increasing Reynolds number for smooth pipes, resulting in lower head loss per unit length. Thus, even without direct pressure data, the trend of increasing Re observed in the experiment logically corresponds to reduced frictional losses within the loop. On the other hand, in the 2-inch hot leg, where the Reynolds number is lower, the contribution of frictional forces is still relatively significant to the total pressure in the system. However, as the Grashof modified number increases, the influence of buoyancy helps reduce the pressure drop effect, as the fluid is naturally driven by the density difference occurring throughout the system. Therefore, the larger pipe diameter in the 2-inch hot leg provides an advantage in increasing the dominance of buoyancy forces while still resulting in a lower Reynolds number value compared to the loop, which affects both the distribution of heat transfer and the pressure drop in the system. Fig. 4 shows that the Reynolds number for flow in the entire loop and the hot leg 2-inch increase significantly with the temperature rise. The flow reaches turbulent conditions in the entire loop at 70°C, with the Reynolds number exceeding 4000. This indicates that the flow in the entire loop has fully transitioned to turbulent flow. This is due to the increased flow velocity and buoyancy forces that drive the transition to turbulence at higher temperatures.

On the other hand, for the hot leg 2-inch, although the Reynolds number approaches the turbulent threshold of 4000 at 90°C, the flow remains in the transition region and has not yet fully reached turbulence. This shows that despite a significant increase in the Reynolds number, the flow in the hot leg 2-inch only begins to show signs of transitioning towards turbulent flow at higher temperatures than the entire loop. One of the main causes of this difference is the pipe diameter. The hot leg 2-inch has a larger diameter compared to the pipes in the entire loop, which contributes to a reduction in flow velocity and increases viscosity, thus delaying the transition to turbulence.

Therefore, although both flows show a consistent increase in Reynolds number as the temperature rises, the flow in the hot leg 2-inch requires higher temperatures to reach turbulent conditions. In contrast, the flow has fully entered the turbulent region at a lower temperature in the entire loop. The relationship between Reynolds data from this experiment and the results of other similar studies is shown in Fig. 6.

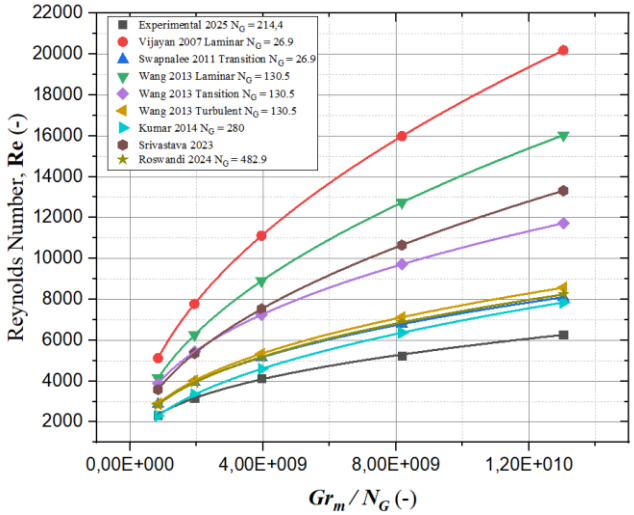

Fig. 6. Comparison of experimental Reynolds number with other studies

Fig. 6 presents the experimental correlation expressed by the Eq. $Re=1.50186(Gr_m/N_G)^{0.35788}$, which links the Reynolds number, Grashof modified number, and the geometric ratio. This correlation shows that the Reynolds number increases as the Grashof modified number divided by the geometrical ratio rises, aligning with the general trend in previous studies. However, this experimental correlation yields higher Reynolds numbers in certain Gasthof modified number-divided geometrical ratio ranges compared to earlier research's theoretical or numerical models.

When compared to earlier studies, such as those by Vijayan for laminar and turbulent flow, Swapnalee for transitional conditions, and Wang [21], who categorized the results into laminar, transition, and turbulent conditions, it is evident that although all models show a similar trend, the experimental correlation produces different outcomes. Furthermore, the graph includes results for various N_G values. For instance, Kumar [8] used $N_G = 280$, while Roswandi [22] used $N_G = 482.9$. These variations in N_G values influence the relationship between the Grashof modified number divided geometrical ratio and the Reynolds number, with higher N_G values generally resulting in lower Reynolds numbers for the same Grashof modified number divided geometrical ratio value.

A major distinguishing factor of this experiment is its focus on examining the effects of loops with non-uniform diameters. In contrast, previous studies primarily used models with uniform pipe geometries or idealized assumptions. This experiment, however, accounts for variations in pipe diameters, particularly the 2-inch hot leg pipe. The variation in pipe diameter significantly impacts the distribution of buoyancy forces and fluid flow velocity, leading to changes in the flow from laminar to transitional and turbulent states.

Other researchers, such as Vijayan [1] and Wang [21], developed correlations that show faster transitions in systems with uniform pipes. However, in this experiment, the variation in pipe diameter delays the transition, as evidenced by the higher Reynolds numbers observed during the transition and turbulent conditions for a given Grashof modified number divided geometrical ratio range. The results from Kumar and Roswandi also show that a higher geometrical ratio can reduce turbulence, which aligns with the findings in this experiment, which state that variations in pipe diameter influence flow transitions.

When comparing the heat transfer and pressure drop characteristics in natural circulation systems, it is evident that previous studies primarily focused on uniform diameter geometries. Vijayan [1] and Wang [21] both demonstrated faster flow transitions in systems with uniform pipe diameters, which led to more straightforward predictions of heat transfer and pressure drop. These studies assumed a smooth, uniform flow that follows well-established correlations for Reynolds and Grashof modified numbers, making the predictions more reliable for such systems.

However, the flow dynamics become more complex in natural circulation systems with non-uniform diameters, like the 2-inch hot leg pipe used in this experiment. In regions where the diameter is restricted, such as in the hot leg, the velocity increases, which leads to higher local Reynolds numbers and potentially more turbulence. This results in a higher pressure drop across these regions, affecting the overall heat transfer performance. The increase in turbulence, especially in the narrower sections of the pipe, can enhance the heat transfer but at the cost of higher energy losses due to the pressure drop.

The non-uniform diameter in this experiment leads to localized variations in heat transfer and pressure drop. For instance, in the narrower sections of the pipe, there is a localized increase in velocity, which increases the Reynolds number and accelerates the transition from laminar to turbulent flow. As a result, the pressure drop in these sections is higher than in uniform systems, which can complicate the predictions of both Reynolds number and heat transfer efficiency.

In contrast, previous studies with uniform diameters did not account for these localized effects. The simplified assumptions used in their models typically resulted in more stable predictions for

pressure drop and heat transfer, but they could not capture the complexities introduced by varying pipe diameters. Therefore, the discrepancies observed in this experiment, especially when comparing the results to those from Vijayan [1], Swapnalee, and Wang [21], can be attributed to the differences in pipe geometries and the resulting impact on heat transfer and pressure drop characteristics. Empirical relationships of Reynolds numbers are constructed from experimental data in Table 4.

Table 4. Correlation Re Based on Experimental

Researcher	Year	Flow Regime	Re-correlation	Error (%)
Vijayan	2007	Laminar	$0.1768(Gr_m/N_G)^{0.5}$	63
Swapnalee	2011	Transition	$1.216(Gr_m/N_G)^{0.378}$	21
Wang	2013	Laminar	$0.1653(Gr_m/N_G)^{0.493}$	53
		Transition	$0.9833(Gr_m/N_G)^{0.403}$	43
		Turbulent	$0.8422(Gr_m/N_G)^{0.3962}$	23
Kumar	2014	All	$0.2285(Gr_m/N_G)^{0.44844}$	10
Srivastava	2023	All	$0.1948(Gr_m/N_G)^{0.47798}$	45
Roswandi	2024	All	$0.95712(Gr_m/N_G)^{0.38901}$	21

Table 4 compares the Reynolds number correlations from previous studies with the experimental results obtained in this study. These correlations, which were derived from uniform-diameter geometries, exhibit varying degrees of error when applied to the experimental data. Notably, the Vijayan [1] correlation shows the highest error (63%), while the Kumar [8] correlation yields a much smaller error (10%).

The non-uniform diameter used in this experiment, particularly in the 2-inch hot leg, may explain the discrepancies in the Reynolds number predictions. Unlike the previous studies, which used systems with uniform diameters, the non-uniform geometry in this experiment introduces complexity to the flow behaviour. In natural circulation systems, a restricted diameter, especially in the hot leg, significantly affects the velocity profile, pressure drop, and heat transfer efficiency. This localized restriction causes velocity gradients not captured by the simplified assumptions of the uniform flow used in the correlations, leading to errors in the Reynolds number estimation. The 2-inch diameter hot leg plays a crucial role in altering the flow dynamics by accelerating the fluid, which influences the Reynolds number at various points in the system. This non-uniformity creates localized differences in flow characteristics more pronounced in natural circulation, where buoyancy forces drive the fluid. As a result, applying uniform diameter correlations to this non-uniform system can lead to significant prediction errors, as observed in Table 4.

Therefore, it is likely that the high error percentages, particularly with correlations such as Vijayan [1] and Wang [21], can be partially attributed to this geometric difference. The existing correlations derived under the assumption of uniform diameters may not be directly applicable to non-uniform geometries, especially when the hot leg diameter creates localized variations in flow and heat transfer characteristics. The high error values reported in the experiment can thus be explained by the lack of consideration for the non-uniform diameter effects in previous studies. This experimental correlation offers a more realistic approach, considering the effect of varying pipe diameters, which mirrors real-world conditions where fluid flow systems often involve pipes of different sizes. By incorporating this factor, the experimental correlation results in slightly higher Reynolds numbers at laminar and transitional flow for a given (Gr_m/N_G) range than Kumar [6], whose predictions rely on idealized or simpler assumptions about flow systems.

Conclusions

The experiment demonstrated that increasing temperature enhances buoyancy forces and mass flow rate, leading to a transition from laminar to turbulent flow, particularly noticeable at temperatures above 70°C. The 2-inch hot leg exhibited superior heat transfer performance compared to smaller diameters, and non-uniform pipe configurations resulted in higher Grashof modified numbers, indicating stronger natural circulation. The developed correlation offers a more accurate prediction of flow behavior in such systems, suggesting that employing a larger hot leg diameter can improve system efficiency, in line with the design characteristics of real-world systems like the AP1000 reactor. However, a limitation of this study is that it focuses on water as a single-phase fluid. Further research could expand on this by incorporating different fluids and geometries, thus broadening the applicability of the findings.

Acknowledgements

This research was supported by the RIIM LPDP Grant and BRIN, grant numbers B811/II.7.5/FR/6/2022 and B103/III.2/HK.04.03/7/2022. We also thank the Research Centre for Nuclear Reactor Technology, the Research Organization for Nuclear Energy, and the National Research and Innovation Agency of Indonesia (BRIN).

References

[1] P. K. Vijayan, M. Sharma, and D. Saha, "Steady state and stability characteristics of single-phase natural circulation in a rectangular loop with different heater and cooler orientations," *Exp Therm Fluid Sci*, vol. 31, no. 8, pp. 925–945, Aug. 2007, doi: 10.1016/j.expthermflusci.2006.10.003.

[2] P. K. Vijayan, A. K. Nayak, D. Saha, and M. R. Gartia, "Effect of loop diameter on the steady state and stability behaviour of single-phase and two-phase natural circulation loops," *Science and Technology of Nuclear Installations*, vol. 2008, 2008, doi: 10.1155/2008/672704.

[3] P. Garibaldi and M. Misale, "Experiments in single-phase natural circulation miniloops with different working fluids and geometries," *J Heat Transfer*, vol. 130, no. 10, Oct. 2008, doi: 10.1115/1.2948393.

[4] M. Misale, "Dynamic behaviour of a rectangular single-phase natural circulation loop: influence of loop inclination," 2010. [Online]. Available: https://www.researchgate.net/publication/268264008

[5] D. Hariyanto, S. Permana, and Suprijadi, "Experimental and simulation approach of the loop geometry effect on the natural circulation system of the advanced nuclear reactor," *Int J Energy Res*, vol. 45, no. 8, pp. 11892–11903, Jun. 2021, doi: 10.1002/er.5903.

[6] M. Misale, J. A. Bocanegra, and A. Marchitto, "Thermo-hydraulic performance of connected single-phase natural circulation loops characterized by two different inner diameters," *International Communications in Heat and Mass Transfer*, vol. 125, Jun. 2021, doi: 10.1016/j.icheatmasstransfer.2021.105309.

[7] B. T. Swapnalee and P. K. Vijayan, "A generalized flow Eq. for single phase natural circulation loops obeying multiple friction laws," *Int J Heat Mass Transf*, vol. 54, no. 11–12, pp. 2618–2629, May 2011, doi: 10.1016/j.ijheatmasstransfer.2011.01.023.

[8] N. Kumar, J. B. Doshi, and P. K. Vijayan, "Investigations on the role of mixed convection and wall friction factor in single-phase natural circulation loop dynamics," *Ann Nucl Energy*, vol. 38, no. 10, pp. 2247–2270, Oct. 2011, doi: 10.1016/j.anucene.2011.06.004.

[9] R. Saha, S. Sen, S. Mookherjee, K. Ghosh, A. Mukhopadhyay, and D. Sanyal, "Experimental and Numerical Investigation of a Single-Phase Square Natural Circulation Loop," *J Heat Transfer*, vol. 137, no. 12, Dec. 2015, doi: 10.1115/1.4030926.

[10] M. Misale, "Experimental study on the influence of power steps on the thermohydraulic behaviour of a natural circulation

loop," Aug. 01, 2016, *Elsevier Ltd*. doi: 10.1016/j.ijheatmasstransfer.2016.04.036.

[11] S. M. Seyyedi, N. Sahebi, A. S. Dogonchi, and M. Hashemi-Tilehnoee, "Numerical and experimental analysis of a rectangular single-phase natural circulation loop with asymmetric heater position," *Int J Heat Mass Transf*, vol. 130, pp. 1343–1357, Mar. 2019, doi: 10.1016/j.ijheatmasstransfer.2018.11.030.

[12] M. Misale, J. A. Bocanegra, D. Borelli, and A. Marchitto, "Experimental analysis of four parallel single-phase natural circulation loops with small inner diameter," *Appl Therm Eng*, vol. 180, Nov. 2020, doi: 10.1016/j.applthermaleng.2020.115739.

[13] D. N. Elton, U. C. Arunachala, and P. K. Vijayan, "Investigations on the dependence of the stability threshold on different operating procedures in a single-phase rectangular natural circulation loop," *Int J Heat Mass Transf*, vol. 161, Nov. 2020, doi: 10.1016/j.ijheatmasstransfer.2020.120264.

[14] S. Bello, P. Gao, and Y. Lin, "Closed-loop experimental investigation of single-phase natural circulation flow phenomena based on temperature and heating power variations," *Ann Nucl Energy*, vol. 151, Feb. 2021, doi: 10.1016/j.anucene.2020.107809.

[15] D. N. Elton, U. C. Arunachala, and P. K. Vijayan, "Stability enhancement in large diameter rectangular natural circulation loops using flow restrictors," *International Communications in Heat and Mass Transfer*, vol. 126, Jul. 2021, doi: 10.1016/j.icheatmasstransfer.2021.105412.

[16] D. N. Elton, U. C. Arunachala, and P. K. Vijayan, "Stabilization of single phase rectangular natural circulation loop of larger diameter using orifice plate," *International Communications in Heat and Mass Transfer*, vol. 137, Oct. 2022, doi: 10.1016/j.icheatmasstransfer.2022.106216.

[17] Westinghouse Electric Company, *AP1000 Design Control Document, Tier 2 Material*, Revision 19, U.S. Nuclear Regulatory Commission, Washington, DC, USA, June 2011.

[18] A. Crabtree and M. Siman-Tov, "Thermophysical properties of saturated light and heavy water for advanced neutron source applications," Oak Ridge National Laboratory, Oak Ridge, TN, USA, Tech. Rep., 1993

[19] B. R. Munson, D. F. Young, and T. H. Okiishi, *Fundamentals of Fluid Mechanics*, 6th ed. Hoboken, NJ: John Wiley & Sons, 2009.

[20] P. K. Vijayan, "Experimental observations on the general trends of the steady state and stability behaviour of single-phase natural circulation loops," 2002. [Online]. Available: www.elsevier.com/locate/nucengdes

[21] J. Y. Wang, T. J. Chuang, and Y. M. Ferng, "CFD investigating flow and heat transfer characteristics in a natural circulation loop," *Ann Nucl Energy*, vol. 58, pp. 65–71, 2013, doi: 10.1016/j.anucene.2013.01.015.

[22] I. Roswandi *et al.*, "Investigation of Natural Circulation Flow Under Steady-State Conditions Using a Rectangular Loop," Teknologi Reaktor Nuklir Tri Dasa Mega vol. 26, no. 2, pp. 77–86, 2024, doi: 10.55981/tdm.2024.7055.